

# Equilibria and dynamics of some aqueous peroxomolybdate catalysts: a $^{17}\text{O}$ NMR spectroscopic study

Fabian Taube,<sup>\*a</sup> Ingegård Andersson,<sup>a</sup> Imre Toth,<sup>b</sup> Andrea Bodor,<sup>b</sup> Oliver Howarth<sup>c</sup> and Lage Pettersson<sup>a</sup>

<sup>a</sup> Department of Chemistry, Inorganic Chemistry, Umeå University, SE-901 87 Umeå, Sweden

<sup>b</sup> Department of Inorganic and Analytical Chemistry, Debrecen University, H 4010 Debrecen, Hungary

<sup>c</sup> Department of Chemistry, University of Warwick, Coventry, UK CV4 7AL

Received 27th June 2002, Accepted 10th October 2002

First published as an Advance Article on the web 25th October 2002

The equilibrium speciation at 278 K and the dynamics in the systems  $p\text{H}^+ + q\text{MoO}_4^{2-} + r\text{H}_2\text{O}_2 + s\text{L} \rightleftharpoons (\text{H}^+)_p(\text{MoO}_4^{2-})_q(\text{H}_2\text{O}_2)_r\text{L}_s$  ( $\text{L} = \text{SO}_4^{2-}$  or  $\text{Cl}^-$ ) in 0.3 M  $\text{Na}_2(\text{SO}_4)$  and 0.6 M  $\text{Na}(\text{Cl})$  medium has been determined from  $^{17}\text{O}$  NMR integral and shift data in the range  $0.7 \leq \text{pH} \leq 4.1$  and at excess of peroxide ( $[\text{H}_2\text{O}_2]_{\text{tot}}/[\text{Mo}]_{\text{tot}} = 3$ ). In 0.3 M  $\text{Na}_2(\text{SO}_4)$  medium species with the following compositions were found:  $\text{MoX}_2^-$  (1,1,2,0),  $\text{MoX}_2$  (2,1,2,0),  $\text{MoX}_2\text{S}^{2-}$  (2,1,2,1),  $\text{MoX}_2\text{S}^-$  (3,1,2,1),  $\text{Mo}_2\text{X}_4^{2-}$  (2,2,4,0),  $\text{Mo}_2\text{X}_4^-$  (3,2,4,0) and  $\text{Mo}_2\text{X}_6^{2-}$  (2,2,6,0), where (Mo) corresponds to  $\text{MoO}_4^{2-}$ , (X) to  $\text{O}_2^{2-}$  or  $\text{HOO}^-$  and (S) to  $\text{SO}_4^{2-}$ . In 0.6 M  $\text{Na}(\text{Cl})$  medium the diperoxomolybdosulfate complex  $\text{MoX}_2\text{S}^-$  is replaced with a novel diperoxomolybdochloride complex  $\text{MoX}_2\text{Cl}^-$  (2,1,2,1), where (Cl) corresponds to  $\text{Cl}^-$ . The numbers in parentheses refer to the values of  $p, q, r$  and  $s$  in the formula above. The stoichiometries of each complex are given by the abbreviated formula  $\text{Mo}_q\text{X}_r\text{S}_s^{(2q+2s-p)-}$  and  $\text{Mo}_q\text{X}_r\text{Cl}_s^{(2q+s-p)-}$ . The following formation constants with  $3\sigma$  were obtained with values for 0.6 M  $\text{Na}(\text{Cl})$  in parenthesis:  $\log \beta_{1,1,2,0} = 11.61$  (11.61);  $\log \beta_{2,1,2,0} = 13.70 \pm 0.10$ ,  $\text{p}K_a = 2.09$  (13.86  $\pm$  0.10,  $\text{p}K_a = 2.25$ );  $\log \beta_{2,1,2,1} = 14.57 \pm 0.07$  (13.87  $\pm$  0.15);  $\log \beta_{3,1,2,1} = 15.27 \pm 0.17$ ,  $\text{p}K_a = 0.70$ ,  $\log \beta_{2,2,4,0} = 24.06 \pm 0.05$  (24.08  $\pm$  0.04);  $\log \beta_{3,2,4,0} = 25.99 \pm 0.18$ ,  $\text{p}K_a = 1.93$  (26.23  $\pm$  0.17,  $\text{p}K_a = 2.15$ );  $\log \beta_{2,2,6,0} = 24.02 \pm 0.15$  (23.9  $\pm$  0.3). The  $\text{p}K_a$  value for  $\text{HSO}_4^-$  was determined to be  $1.06 \pm 0.11$ . At 278 K the  $\text{MoX}_2$  and  $\text{Mo}_2\text{X}_4$  complexes are in chemical exchange and the rate of exchange increases upon protonation. At 312 K there is also measurable exchange between  $\text{MoX}_2\text{S}$  and the  $\text{MoX}_2$  and  $\text{Mo}_2\text{X}_4$  complexes. The dynamics in 0.6 M  $\text{Na}(\text{Cl})$  medium seem to be very similar to those in the sulfate medium.

## Introduction

The catalytic use of peroxometallates is well known and widespread. Several types of diperoxomolybdates, including monomeric complexes with  $1-4$  or without different organic ligands, *i.e.*  $[\text{MoO}(\text{O}_2)_2(\text{OH})(\text{H}_2\text{O})]^-$  and  $[\text{MoO}(\text{O}_2)_2(\text{H}_2\text{O})]^{5-7}$  and dimeric complexes, *i.e.*  $[\text{O}[\text{MoO}(\text{O}_2)_2(\text{H}_2\text{O})]_2]^{2-}$ ,<sup>8,9</sup> are being used as catalysts in oxidation reactions of different organic substrates. Recent studies have shown that a catalytic amount of molybdate can be used as an activator for hydrogen peroxide in the bleaching step of paper pulp.<sup>10-12</sup> The active complexes at excess of peroxide in the bleaching step are believed to be monomeric molybdates with two peroxo groups coordinated to the molybdenum atom.<sup>13</sup> It has been shown that the oxidizing ability of monomeric diperoxometallates depends largely upon the strength of the O–O bond, *i.e.* complexes with weaker O–O bonds generally are more reactive as oxidizing agents.<sup>14,15</sup> Apart from the type of transition metal, the O–O bond strength is also dependent on the nature of the other coordinated ligands. Griffith<sup>16</sup> has for example shown that the  $\nu_1(\text{O}-\text{O})$  stretching frequency increases on increasing the electronegativity on the Mo-atom by attachment of fluoride. In fact, the nature of the coordinated ligands in affecting the one-electron-oxidizing ability of different diperoxometallates has been proposed to be of greater importance than the nature of the metal itself.<sup>15</sup>

In order to study the catalytic properties of a specific complex in solution it is essential to know the composition and the distribution of the complex in the solution of interest. This is especially important when several different complexes co-exist in a solution. The present speciation study draws on a preceding potentiometric and  $^{95}\text{Mo}$  NMR study of peroxomolybdates

in 0.3 M  $\text{Na}_2(\text{SO}_4)$  medium, in which sulfate was found to coordinate to molybdate in the presence of hydrogen peroxide.<sup>13</sup> The aim of the present study was to investigate some of the complexes that could not be satisfactorily verified in the potentiometric study, but also to investigate the interaction of chloride with peroxomolybdates, since chloride is a commonly used medium anion in solution studies. Similarly to earlier studies on peroxomolybdosulfate complexes,<sup>17-19</sup> chloride interaction on peroxomolybdates has been found only in acidic solutions, including monomeric complexes, *i.e.*  $[\text{MoO}(\text{O}_2)\text{Cl}_2]^{20}$ ,  $[\text{MoO}(\text{O}_2)\text{Cl}_4]^{2-21}$  and dimeric complexes, *i.e.*  $[\text{Mo}_2\text{O}_2(\text{O}_2)_4\text{Cl}_2]^{2-21}$ .

The present study investigates the equilibrium and dynamics of the peroxomolybdate system at excess of peroxide in two different media, 0.3 M  $\text{Na}_2(\text{SO}_4)$  and 0.6 M  $\text{Na}(\text{Cl})$ , by means of  $^{17}\text{O}$  NMR spectroscopy.

## Experimental

### Chemicals

The molybdate stock solutions, sulfuric acid solutions and the disodium sulfate were prepared according to reference 22. The hydrochloric acid stock solution was prepared from concentrated hydrochloric acid. Sodium chloride (E. Merck) was dried at 180 °C and used without further purification. Hydrogen peroxide stock solutions were prepared from 30 % (9.7 M) hydrogen peroxide (E. Merck p.a.) and used without further standardization.  $^{17}\text{O}$  enriched hydrogen peroxide was prepared from  $\text{H}_2\text{O}$  enriched to 12.3% in  $^{17}\text{O}$  by trapping the product of an electrical discharge.<sup>23</sup>

## Solutions for EMF and NMR studies

The solutions for the EMF and NMR studies were prepared from stock solutions at 298 K, to contain 300 mM molybdate and 900 mM peroxide at pH *ca.* 4. Each of these solutions was then titrated with small amounts of sulfuric acid (hydrochloric acid) down to pH *ca.* 0.7. The ionic medium was kept constant during the titrations by addition of disodium sulfate (sodium chloride). In all preparation of solutions distilled water was used. To avoid possible decomposition of peroxide in the solutions during preparation<sup>13</sup> the sulfuric acid (hydrochloric acid) was always added prior to the addition of hydrogen peroxide.

**EMF measurements.** The pH value of each solution was measured on separate solutions with an Orion Research 8103 Ross combination electrode at 298 and 278 K respectively. The electrode was calibrated against buffer solutions of known  $[H^+]$ , at the two different temperatures respectively. Thus, all pH measurements are on the concentration scale, where  $-\log [H^+] = \text{pH}$ .

**NMR measurements.** NMR measurements were made on solutions at 298 K and 278 K in 0.3 M  $\text{Na}_2(\text{SO}_4)$  and 0.6 M  $\text{Na}(\text{Cl})$  medium. For the dynamic NMR, complementary measurements on solutions at 288, 312 and 322 K were also made.  $^{17}\text{O}$  NMR spectra were recorded at 67.8 MHz on a Bruker DRX 500 MHz spectrometer. Typically, pulse width = 10  $\mu\text{s}$  (appr.  $40^\circ$ ), pulse repetition time = 0.1 s, spectral widths of 1200 ppm (81.4 kHz) were used, and data for the FID were accumulated in 8k blocks. Spectra were integrated after baseline correction. The deconvolution subroutine of the software program, 1D WINNMR (Bruker, version 950901.0) was used. Enrichment of the oxygens to 3% was done by addition of  $\text{H}_2^{17}\text{O}$  (12 atom %  $^{17}\text{O}$ , Cambridge Isotope Laboratories) to the samples. The peroxide oxygens, as well as the sulfate oxygens, were not involved in the  $^{17}\text{O}$  isotope enrichment, being inert to oxygen exchange. However, for some samples the peroxide oxygens were enriched to 12% by addition of  $\text{H}_2^{17}\text{O}_2$ . Chemical shifts refer to the signal of tap water,  $\delta$  0. Longitudinal relaxation times,  $T_1$ , of the different species are in the range 1–10 ms. Thus 100 ms relaxation delays used for acquisition are good enough for quantitative integration of the peaks. Evaluation of the 2D EXSY spectra (Fig. 6) was made by the matrix formulated eqn. (1).

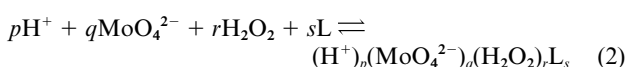
$$A = e^{-R\tau_m} \quad (1)$$

where  $A$  is the matrix of the normalized volume integrals,  $R$  is the matrix of the rate constants and relaxation rates, and  $\tau_m$  is the mixing time.<sup>24</sup>

## NMR data

In the  $\text{H}^+ - \text{MoO}_4^{2-} - \text{H}_2\text{O}_2 - \text{SO}_4^{2-}$  system 16 spectra were recorded in the ranges  $0.70 \leq \text{pH} \leq 4.0$ ,  $40 \leq [\text{Mo}]_{\text{tot}}/\text{mM} \leq 300$ ,  $120 \leq [\text{H}_2\text{O}_2]_{\text{tot}}/\text{mM} \leq 900$  and  $152 \leq [\text{SO}_4^{2-}]_{\text{tot}}/\text{mM} \leq 555$ . In the  $\text{H}^+ - \text{MoO}_4^{2-} - \text{H}_2\text{O}_2 - \text{Cl}^-$  system eight spectra were recorded in the ranges  $0.74 \leq \text{pH} \leq 4.2$ ,  $49.2 \leq [\text{Mo}]_{\text{tot}}/\text{mM} \leq 300$ ,  $147 \leq [\text{H}_2\text{O}_2]_{\text{tot}}/\text{mM} \leq 900$  and  $300 \leq [\text{Cl}^-]_{\text{tot}}/\text{mM} \leq 800$ .

**Data treatment.** The equilibria are written in terms of the components  $\text{H}^+$ ,  $\text{MoO}_4^{2-}$ ,  $\text{H}_2\text{O}_2$ ,  $\text{SO}_4^{2-}$  (or  $\text{Cl}^-$ ), according to reaction (2)



where L is either  $\text{SO}_4^{2-}$  or  $\text{Cl}^-$ . The formation constants are denoted  $\beta_{p,q,r,s}$  and the stoichiometry of each complex is given both in the notation  $(p,q,r,s)$  and by the abbreviated formula  $\text{Mo}_q\text{X}_r\text{S}_s^{(2q+2s-p)}$  ( $\text{Mo}_q\text{X}_r\text{Cl}_s^{(2q+s-p)}$ ), where (Mo) corre-

sponds to  $\text{MoO}_4^{2-}$ , (X) to  $\text{O}_2^{2-}$  or  $\text{HOO}^-$ , (S) to  $\text{SO}_4^{2-}$  and (Cl) to  $\text{Cl}^-$ . In the least squares computer program LAKE,<sup>25</sup> formation constants for arbitrary but systematically chosen complexes  $(\text{H}^+)_p(\text{MoO}_4^{2-})_q(\text{H}_2\text{O}_2)_r\text{L}_s$  are varied, so that the sum of error squares,  $U = \sum (W_i \Delta A_i)^2$ , is minimized. The set of complexes giving the lowest  $U$ -value forms the model, which best explains the experimental data.  $A_i$  can be either the total concentration of components, concentration of complexes, NMR peak integrals or chemical shifts.  $W_i$  is a weighting factor for the different types of data. In this study we have used a weighting factor that gives NMR peak integrals a predominant contribution to the sum of residuals. Modelling and construction of distribution diagrams were performed using the computer program WINSGW,<sup>26</sup> a program package for equilibrium calculations based on the SOLGASWATER algorithm.<sup>27</sup>

## Results and discussion

### Equilibrium calculations

A prerequisite for the quantitative use of peak integrals is well-separated signals. As can be seen from Fig. 1, a typical  $^{17}\text{O}$

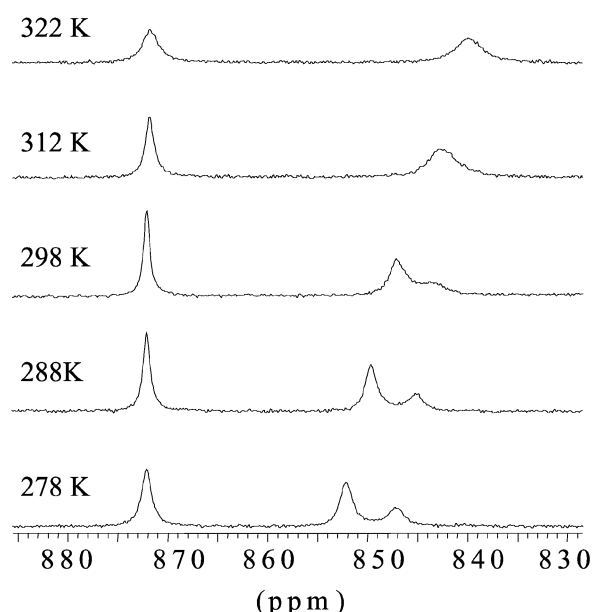


**Fig. 1** Temperature dependence of the terminal oxygen signals at pH 2.15 in 0.3 M  $\text{Na}_2(\text{SO}_4)$  medium.  $[\text{Mo}]_{\text{tot}} = 194$  mM,  $[\text{H}_2\text{O}_2]_{\text{tot}} = 582$  mM and  $[\text{SO}_4^{2-}]_{\text{tot}} = 268$  mM.

NMR spectrum at 298 K reveals a broad unresolved signal just below 850 ppm, arising from the terminal oxygen atoms in the  $\text{MoX}_2$  and  $\text{Mo}_2\text{X}_4$  complexes. Due to slower exchange it splits into two separate signals when the temperature is decreased to 278 K. In order to make reliable assignments and obtain accurate integral and chemical shift data in both systems, experimental data were collected at 278 K. A few experiments made with  $\text{H}_2^{17}\text{O}_2$  also revealed a very broad peroxo signal in which the chemical shifts for different peroxo groups were not distinguishable, except for a narrow signal superimposed on the broad signal (Fig. 2). The choice of terminal oxygen signals for quantitative analyses was advantageous because of the relatively narrow and well-separated signals. The assignment of the different signals was made by recording spectra at different sulfate (chloride) and molybdate concentrations.

**Sulfate system.** As a basis for the calculation of the formation constants, a potentiometric study in the ranges  $2.0 \leq \text{pH} \leq 5.5$ ,  $5.00 \leq [\text{Mo}]_{\text{tot}}/\text{mM} \leq 80.00$  at 298 K in 0.300 M  $\text{Na}_2(\text{SO}_4)$

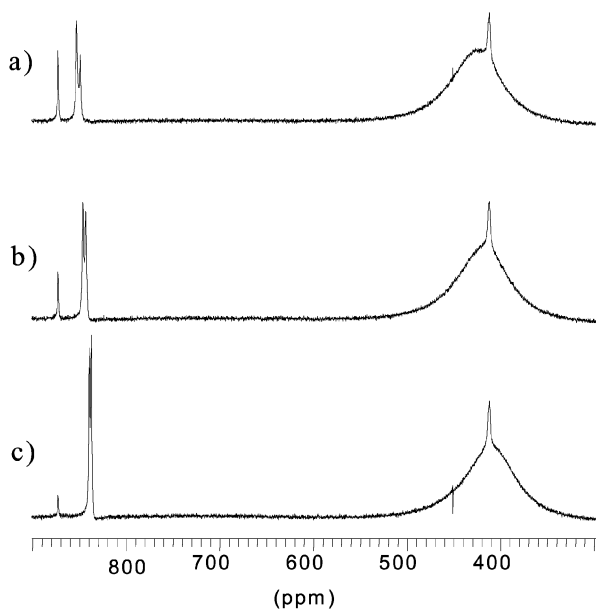


**Fig. 2** pH-dependence of the peroxy signals in 0.3 M Na<sub>2</sub>(SO<sub>4</sub>) medium at 278 K. [Mo]<sub>tot</sub> = 300 mM, [H<sub>2</sub>O<sub>2</sub>]<sub>tot</sub> = 900 mM. (a) pH 2.3, (b) pH 2.6 and (c) pH 3.0.

medium was used.<sup>13</sup> Based on this study, at least three different types of complexes could be expected at excess of peroxide (H<sub>2</sub>O<sub>2</sub>/Mo > 2), namely monomeric diperoxomolybdates (p,1,2,0), p = 1–2, monomeric diperoxomolybdsulfates (p,1,2,1) p = 2–3, and dimeric diperoxomolybdates (p,2,4,0) p = 2–3. However, due to the limited pH- and molybdate concentration ranges studied, the protonated dimer (3,2,4,0) and sulfate (3,1,2,1) complexes could not be verified by potentiometry. In the present study, experimental data down to pH 0.70 and up to 300 mM in total molybdate concentrations have been used in order to fully characterize these complexes. The formation constants for the acidic (3,1,2,1) and (3,2,4,0) complexes are however dependent on the pK<sub>a</sub> value for HSO<sub>4</sub><sup>-</sup> and the total concentration of sulfate. A small error in either of them will result in comparatively high errors for the acidic data points and thereby in a less accurate formation constant. Therefore, higher 3σ values for log β<sub>3,1,2,1</sub> and log β<sub>3,2,4,0</sub> can be expected in the calculations. The final model is presented in Table 1, and the distribution of the proposed complexes at 300 mM molybdate as a function of pH is presented in Fig. 3a.

The chemical shift curves in Fig. 4a indicate that only MoX<sub>2</sub><sup>-</sup> and Mo<sub>2</sub>X<sub>4</sub><sup>2-</sup> can be protonated, although the model suggests a protonation step for the peroxomolybdsulfate complex, MoX<sub>2</sub>S<sup>2-</sup> (2,1,2,1), as well. This implies that the protonation of (2,1,2,1) occurs at a very distant sulfate oxygen and so does not affect the chemical shift for the terminal oxygen (δ<sub>O</sub> 873). A further signal at δ<sub>O</sub> 841 with no change in chemical shift over the measured pH interval was also found. As can be seen from Fig. 5, this signal can be discerned from pH 4.0 to 2.15. Its relative area depends on the total concentration of molybdate in the same way as the dimeric Mo<sub>2</sub>X<sub>4</sub> complexes and decreases with decreasing pH. In the calculations this signal could be explained by a Mo<sub>2</sub>X<sub>6</sub><sup>2-</sup> (2,2,6,0) complex. This composition is in accordance with the crystal structure found by Le Carpentier *et al.*<sup>28</sup> and Mitschler *et al.*,<sup>29</sup> having four side-on (η<sup>2</sup>) peroxy groups, two terminal oxygens and two bridging hydroperoxy (OOH) groups. The absence of a chemical shift change for the terminal oxygen signal in this pH-interval can be explained by the fact that there are no likely protonation sites on this complex, since the hydroperoxy groups cannot be protonated. The presence of a complex containing hydroperoxy groups can also explain the narrow peroxy signal (δ<sub>O-O</sub> 412) found in H<sub>2</sub><sup>17</sup>O<sub>2</sub>

**Table 1** Composition, formation constants (log β) and <sup>17</sup>O NMR shifts for peroxomolybdates in 0.3 M Na<sub>2</sub>(SO<sub>4</sub>) media at 278 K. (1,1,2,0) is “locked”, the others are optimized

<i>p,q,r,s</i>	Notation	log β (3σ)	pK <sub>a</sub>	Shift/ppm
1,0,0,1	HSO <sub>4</sub> <sup>-</sup>	1.06 (11)	1.06	
2,1,2,1	MoX <sub>2</sub> S <sup>2-</sup>	14.57 (7)		872.6
3,1,2,1	MoX <sub>2</sub> S <sup>-</sup>	15.27 (17)	0.70	872.6
1,1,2,0	MoX <sub>2</sub> <sup>-</sup>	11.61		834.1
2,1,2,0	MoX <sub>2</sub>	13.70 (10)	2.09	872.8
2,2,4,0	Mo <sub>2</sub> X <sub>4</sub> <sup>2-</sup>	24.06 (5)		832.9
3,2,4,0	Mo <sub>2</sub> X <sub>4</sub> <sup>-</sup>	25.99 (18)	1.93	868.5
2,2,6,0	Mo <sub>2</sub> X <sub>6</sub> <sup>2-</sup>	24.02 (15)		840.8

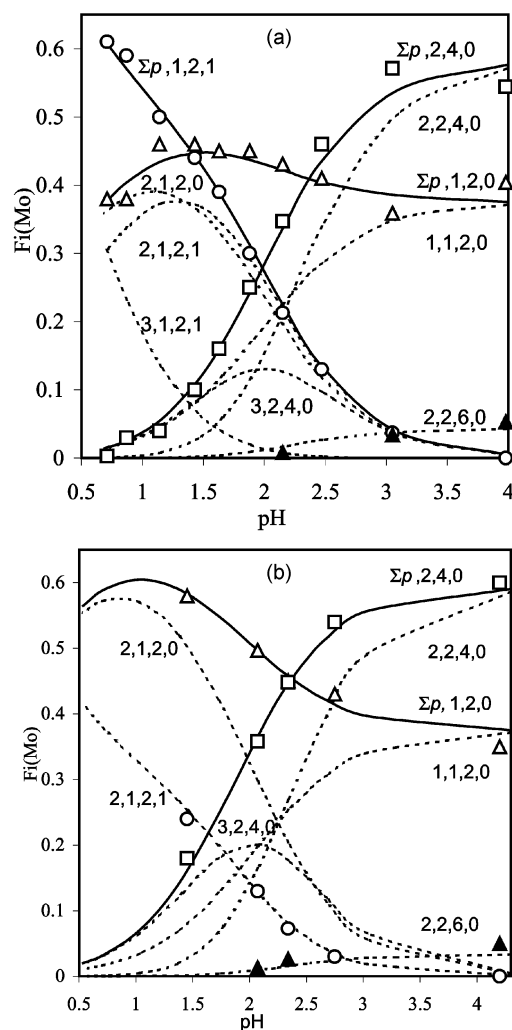


**Fig. 3** Distribution diagrams plotted as  $F_i$  versus pH.  $F_i$  is defined as the ratio between [Mo] in a species and [Mo]<sub>tot</sub> in solution. Full-drawn curves represent the sum of each type of complex, while the distribution of a single complex is shown by dashed curves. The symbols represent experimental NMR data points. In order to compare the experimental data points with the model the diagrams are calculated with varying total concentrations of the components, according to the experimental data points: (a) 0.3 M Na<sub>2</sub>(SO<sub>4</sub>) medium, 278 ≤ [Mo]<sub>tot</sub>/mM ≤ 300, 834 ≤ [H<sub>2</sub>O<sub>2</sub>]<sub>tot</sub>/mM ≤ 900 and 152 ≤ [SO<sub>4</sub><sup>2-</sup>]<sub>tot</sub>/mM ≤ 555. (b) 0.6 M NaCl medium, 283 ≤ [Mo]<sub>tot</sub>/mM ≤ 300, 849 ≤ [H<sub>2</sub>O<sub>2</sub>]<sub>tot</sub>/mM ≤ 900, 300 ≤ [Cl]<sub>tot</sub>/mM ≤ 850.

enriched samples, which in contrast to the broad peroxy signal does not change its chemical shift within the measured pH interval (Fig. 2). Unfortunately, this signal was difficult to evaluate because the integral of the broad signal was underestimated. The relatively high uncertainty in the form-

**Table 2** Composition and formation constants ( $\log \beta$ ) in 0.3 M  $\text{Na}_2(\text{SO}_4)$  media at 298 K determined by potentiometry

$p,q,r,s$	Notation	$\log \beta \pm 3\sigma$	$pK_a$
1,0,0,1	$\text{HSO}_4^-$	$1.27 \pm 0.03^b$	1.27
1,1,2,0	$\text{MoX}_2^-$	$11.61 \pm 0.03^a$	—
2,1,2,0	$\text{MoX}_2^-$	$13.77 \pm (0.06)^a$	2.16
2,1,2,1	$\text{MoX}_2\text{S}^{2-}$	$14.50 \pm (0.06)^a$	—
2,2,4,0	$\text{Mo}_2\text{X}_4^{2-}$	$23.77 \pm (0.11)^a$	—

<sup>a</sup> Ref. 13. <sup>b</sup> Ref. 22.

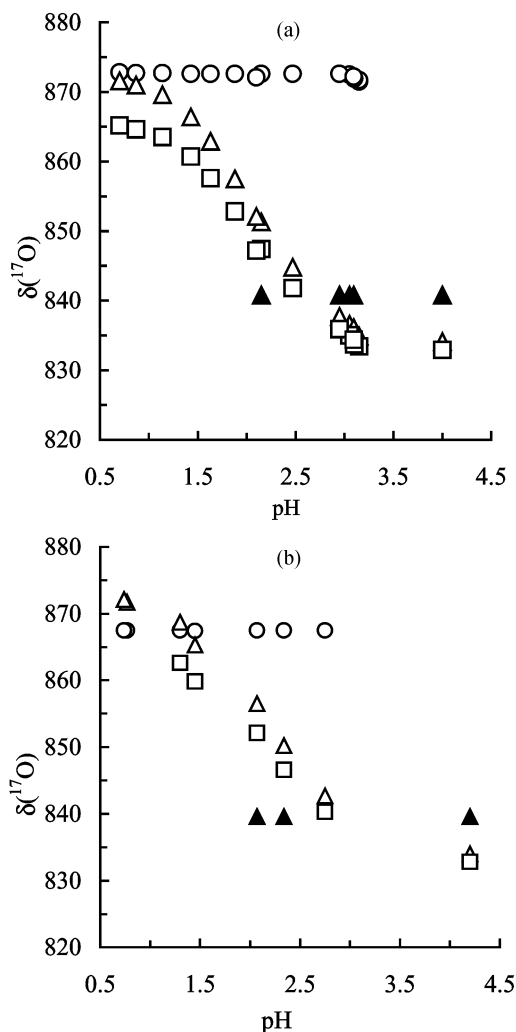


**Fig. 4**  $^{17}\text{O}$  NMR chemical shifts of terminal oxygen signals at 278 K as a function of pH from solutions with  $\text{H}_2\text{O}_2/\text{Mo} = 3$  in (a) 0.3 M  $\text{Na}_2(\text{SO}_4)$  medium,  $\text{Mo}_2\text{X}_4$  ( $\square$ ),  $\text{MoX}_2$  ( $\triangle$ ),  $\text{MoX}_2\text{S}$  ( $\circ$ ),  $\text{Mo}_2\text{X}_6$  ( $\blacktriangle$ ) and (b) 0.6 M  $\text{Na}(\text{Cl})$  medium,  $\text{Mo}_2\text{X}_4$  ( $\square$ ),  $\text{MoX}_2$  ( $\triangle$ ),  $\text{MoX}_2\text{Cl}$  ( $\circ$ ),  $\text{Mo}_2\text{X}_6$  ( $\blacktriangle$ ).

ation constant of the (2,2,6,0) complex, especially in 0.6 M  $\text{Na}(\text{Cl})$  medium, is partly due to its small contribution, but mostly due to the low number of experimental data points in which the corresponding terminal oxygen signal could be evaluated.

Compared with the potentiometric data at 298 K (Table 2) the  $pK_a$  of  $\text{HSO}_4^-$  is 0.21 units lower and the  $pK_a$  of (2,1,2,0) is 0.07 units lower at 278 K. On the other hand, the dimeric (2,2,4,0) complex is stronger, as indicated by the higher dimerization constant,  $K_d$ , at 278 K, compared with 298 K (Table 3). This is probably a direct consequence of the decrease in temperature, which in general favours di- and polynuclear complexes. The finding of a (2,2,6,0) complex at 278 K is however probably not temperature related. It is unlikely that the

**Table 3** Dimerization constants ( $\log K_d$ ) for the (2,2,4,0) complex in different media and at different temperatures

Medium	$T/\text{K}$	$\log K_d^a$
0.6 M $\text{Na}(\text{Cl})$	278	0.86
0.3 M $\text{Na}_2(\text{SO}_4)$	278	0.84
0.3 M $\text{Na}_2(\text{SO}_4)$	298	$0.55^b$

<sup>a</sup> Defined as:  $\log K_d = \log \beta_{2,2,4,0} - 2(\log \beta_{1,1,2,0})$ . <sup>b</sup> Ref. 13.

**Table 4** Composition, formation constants ( $\log \beta$ ) and  $^{17}\text{O}$  NMR shifts for peroxomolybdates in 0.6 M  $\text{Na}(\text{Cl})$  media at 278 K. (1,1,2,0) is “locked”, the others are optimized

$p,q,r,s$	Notation	$\log \beta (3\sigma)$	$pK_a$	Shift/ppm
2,1,2,1	$\text{MoX}_2\text{Cl}^-$	13.87 (15)	—	867.5
1,1,2,0	$\text{MoX}_2^-$	11.61	—	834.0
2,1,2,0	$\text{MoX}_2$	13.86 (10)	2.25	872.1
2,2,4,0	$\text{Mo}_2\text{X}_4^{2-}$	24.08 (4)	—	832.9
3,2,4,0	$\text{Mo}_2\text{X}_4^-$	26.23 (17)	2.15	869.7
2,2,6,0	$\text{Mo}_2\text{X}_6^{2-}$	23.9 (3)	—	839.6

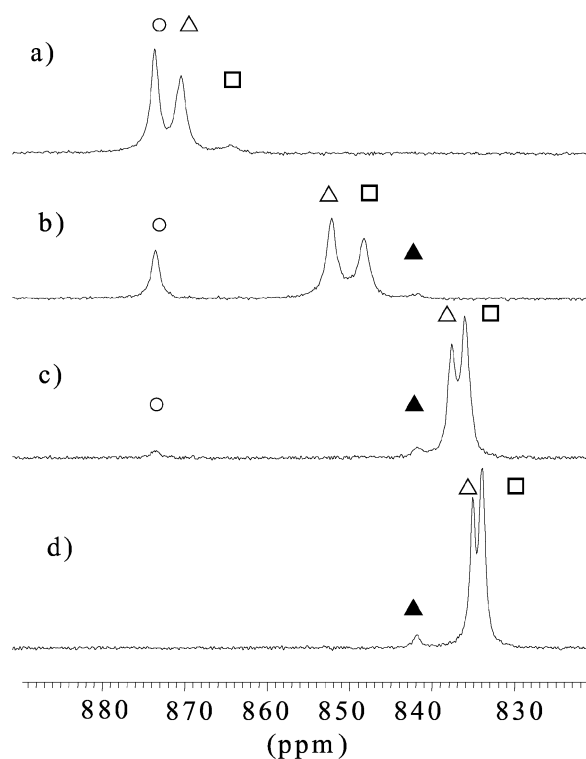


**Fig. 5** pH-dependence of the terminal oxygen signals at 278 K in 0.3 M  $\text{Na}_2(\text{SO}_4)$  medium and  $\text{H}_2\text{O}_2/\text{Mo} = 3$ . pH (a) 1.14, (b) 2.15, (c) 3.05 and (d) 4.0.  $\text{Mo}_2\text{X}_4$  ( $\square$ ),  $\text{MoX}_2$  ( $\triangle$ ),  $\text{MoX}_2\text{S}$  ( $\circ$ ),  $\text{Mo}_2\text{X}_6$  ( $\blacktriangle$ ).

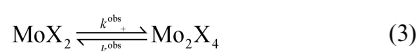
(2,2,6,0) complex exists at the low molybdate concentration used in the potentiometric study.

**Chloride system.** The speciation in 0.6 M  $\text{Na}(\text{Cl})$  medium at excess of peroxide contains a novel dperoxomolybdochloride (2,1,2,1) complex  $\text{MoX}_2\text{Cl}^-$  in addition to the monomeric and dimeric complexes (Table 4 and Fig. 3b). In contrast to  $\text{MoX}_2\text{S}^{2-}$ ,  $\text{MoX}_2\text{Cl}^-$  does not seem to protonate. This would otherwise definitely have been revealed by a chemical shift change, since there is no “distant” oxygen that can be protonated in this complex. As can be seen from Fig. 4b, there is no change in chemical shift for this signal. Furthermore, the dis-

tribution diagrams in Fig. 3 show that  $\text{MoX}_2\text{S}^{2-}$  and  $\text{MoX}_2\text{Cl}^-$  both start to form at about pH 4, but that  $\text{MoX}_2\text{Cl}^-$  never predominates, in contrast to  $\text{MoX}_2\text{S}^{2-}$  and  $\text{MoX}_2\text{S}^-$ . The difference in strength between the  $\text{MoX}_2\text{S}$  complexes and the  $\text{MoX}_2\text{Cl}^-$  complex is even more pronounced than indicated by the distribution diagrams, because the total concentration of sulfate at a given pH-value always is lower than the total concentration of chloride. Furthermore, the stronger sulfate complexes suppress the other acidic complexes. This is reflected in the formation constants for  $\text{MoX}_2$  (2,1,2,0) and  $\text{Mo}_2\text{X}_4^-$  (3,2,4,0), which are lower in 0.3 M  $\text{Na}_2(\text{SO}_4)$  medium than in 0.6 M  $\text{NaCl}$  medium. The pH range of formation indicates that  $\text{MoX}_2\text{S}^{2-}$  forms *via* a condensation reaction between either  $\text{MoX}_2$  (2,1,2,0) and sulfate, or  $\text{MoX}_2^-$  (1,1,2,0) and hydrogen sulfate, whereas the formation of  $\text{MoX}_2\text{Cl}^-$  occurs *via* a reaction through  $\text{MoX}_2$  (2,1,2,0) rather than through  $\text{MoX}_2^-$  (1,1,2,0). According to Shoemaker *et al.*<sup>30</sup> the structure of  $\text{MoX}_2$  (2,1,2,0) contains two water groups. Presumably, one of the water groups is replaced by the chloride ion. In solutions with a very high concentration of chloride ions ( $\geq 4.78$  M), and low concentration of molybdate ( $\leq 1$  mM), an uncharged  $\text{MoXCl}_2$  (4,1,1,2) complex, together with the  $\text{MoX}_2$  (2,1,2,0) complex, have been proposed to be the only complexes at excess of peroxide. Here one of the peroxy groups in the  $\text{MoX}_2$  (2,1,2,0) complex is replaced by two chloride ions, even at high excess of peroxide.<sup>20</sup> In the present study, where the concentration of chloride ions in the NMR solutions is comparatively low, there is no indication of such a complex.

### Equilibrium dynamics

The spectrum at 298 K in Fig. 1 shows a relatively narrow signal at  $\delta_{\text{O}}$  871.4 assigned to the time averaged signal (line width,  $\text{LW} = 50$  Hz) of the 2,1,2,1 and 3,1,2,1 complexes, and two exchange broadened signals at  $\delta_{\text{O}}$  848.9 and 844.5 attributed to the 1,1,2,0 and 2,1,2,0 monomers ( $\text{LW} = 123$  Hz) and 2,2,4,0 and 3,2,4,0 dimers ( $\text{LW} \sim 180$  Hz) respectively, being also in fast proton exchange. On decreasing the temperature to 288 K, all signals shift slightly to lower field and the signal of the sulfate complexes broadens slightly ( $\text{LW} = 58$  Hz) as expected for any quadrupolar  $^{17}\text{O}$  NMR signal recorded in a more viscous solution. In contrast, the signals of the monomer and dimer complexes narrow to 91 and 120 Hz, respectively. This kind of narrowing is typical for systems in a slow exchange regime on the NMR time scale. The change in the line widths of these two signals is in fact a combination of the relaxation broadening and the narrowing that arises from slowing the chemical exchange. Unfortunately, there is no simple method to separate the two effects. At 278 K the signals from the sulfate complexes behave similarly ( $\text{LW} = 81$  Hz) but the viscosity effect for the other two signals seems to be somewhat larger than the effect of slower chemical exchange, resulting in a small net line broadening ( $\text{LW} = 99$  and 127 Hz, respectively). On increasing the temperature to 312 K and 322 K, the chemical exchange between the monomers and dimers is fast enough to convert the system to a fast exchange regime, but this time averaged signal ( $\delta_{\text{O}}$  840.3,  $\text{LW} = 298$  and  $\delta_{\text{O}}$  837,  $\text{LW} = 222$  Hz, respectively) is still separated from the signal of the sulfate complexes. However, this signal ( $\delta_{\text{O}}$  869.5, and 868.8) seems to be involved in chemical exchange with the other complexes at higher temperature, for it shows  $\text{LW} = 77$  and 135 Hz at 312 and 322 K, respectively. Unfortunately, because the effects of the exchange and the viscosity related relaxation on the line shape cannot easily be separated, a fully quantitative analysis of the exchange system cannot be made. However, we have a two-site exchange system involving the monomer and the dimer complexes at 288 K (eqn. (3)):



where  $k_{\text{obs}}^+$  and  $k_{\text{obs}}^-$  are the pseudo first order rate constants of the dimerisation and the reverse reaction. If we take the measured line width of the sulfate complexes as a non exchange line width ( $\text{LW}^0$ ) and suppose that this value is similar for the structurally related monomer and dimer complexes, we may estimate the rate constants, as  $k_{\text{obs}} = \pi \text{LB}$ , where the line broadening,  $\text{LB} = \text{LW} - \text{LW}^0$ . At 278 K,  $k_{\text{obs}}^+ = \pi \times (99 - 81) = 57 \text{ s}^{-1}$  and  $k_{\text{obs}}^- = \pi \times (127 - 81) = 145 \text{ s}^{-1}$ . Another way to interpret these constants is to use  $\tau = 1/k_{\text{obs}}$  as a lifetime of complexes in a given chemical system. For example, the life time of a  $\text{Mo}=\text{O}$  entity in the dimer at 278 K,  $\tau = 1/k_{\text{obs}}^- = 7$  ms. This conditional life time can be substantially shorter in more acidic solution, as exemplified in Fig. 5; the spectrum at pH 3.05 shows much narrower signals of the monomers and dimers, than that at pH 2.15. This implies that protonation of the monomeric and dimeric complexes increase the rate of the chemical exchange of the  $\text{Mo}=\text{O}$  entity. The exchange reactions can also be detected by  $^{17}\text{O}$  2D EXSY. A sample consisting of 200 mM molybdate, 600 mM peroxide and 270 mM sulfate, at pH = 2 and 278 K, shows a cross peak between the monomer and dimer and absence of any such peak to the sulfate species (Fig. 6). This indicates a two-site exchange system in

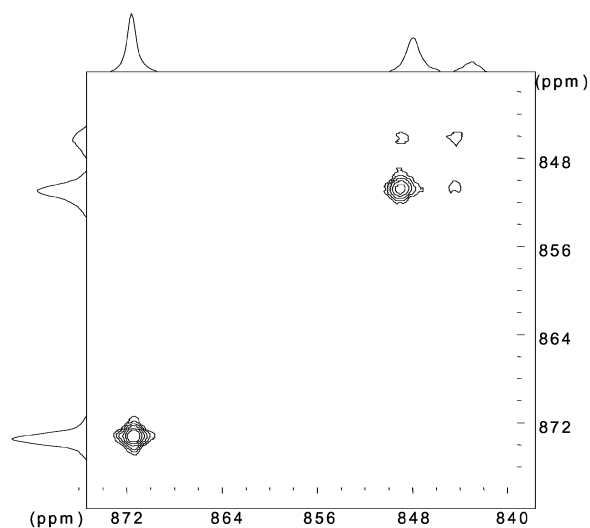


**Fig. 6**  $^{17}\text{O}$  2D EXSY spectra of terminal oxygen signals in 0.3 M  $\text{Na}_2(\text{SO}_4)$  medium.  $[\text{Mo}]_{\text{tot}} = 200$  mM,  $[\text{H}_2\text{O}_2]_{\text{tot}} = 600$  mM,  $[\text{SO}_4^{2-}]_{\text{tot}} = 270$  mM at pH = 2.0 and 278 K;  $\tau_{\text{m}} = 3$  ms.

accordance with the line shape analysis (see above). By recording 2D EXSY spectra at three different mixing times (6  $\mu\text{s}$ , 3 ms and 6 ms) and analyzing the volume integral *vs.* mixing time curve, the pseudo first order rate constants of the exchange reaction, defined by eqn. 1, can be calculated. Values of  $k_{\text{obs}}^+ = 65$  or  $55 \text{ s}^{-1}$  and  $k_{\text{obs}}^- = 175$  or  $142 \text{ s}^{-1}$  have been computed from the spectra at  $\tau_{\text{m}} = 3$  or 6 ms, respectively. These values slightly differ, indicating the uncertainties attributed to the volume integrals. However, the principle of microscopic reversibility for the two site system is acceptably fulfilled, namely  $k_{\text{obs}}^+ p_{\text{mono}} = 48 \text{ s}^{-1} \cong k_{\text{obs}}^- p_{\text{dimer}} = 46 \text{ s}^{-1}$  and  $k_{\text{obs}}^+ p_{\text{mono}} = 41 \text{ s}^{-1} \cong k_{\text{obs}}^- p_{\text{dimer}} = 37 \text{ s}^{-1}$  for the two different mixing times, respectively ( $p_{\text{mono}} (= 0.74)$  and  $p_{\text{dimer}} (= 0.26)$  are the molar fractions of the species, measured by integration of the 1D  $^{17}\text{O}$  NMR peaks). If we take the average values of the rate constant, *i.e.*  $k_{\text{obs}}^- \cong 159 \text{ s}^{-1}$ , we can calculate the average life time of the dimer,  $\tau = 1/k_{\text{obs}}^- = 6$  ms. Although this life time is almost the same as the life time calculated from line broadening data,  $1/k_{\text{obs}}^- = 7$  ms, the slightly shorter life time at pH 2.0 compared to 2.15 fits the conclusions from the pH dependent line broadening (Fig. 5).

One can compare the labilities of the monomers and dimers to the same properties of the sulfate complexes. The latter are more inert, being less broadened even at lower pH values, as

shown in Fig. 5. However, there is a measurable exchange reaction between the sulfate complexes and the other two complexes above room temperature, as seen in Fig. 1. Finally, the dynamics in the chloride medium seem to be very similar to those in the sulfate medium.

## Conclusions

This study has shown that  $^{17}\text{O}$  NMR chemical shifts and integrals of terminal oxygen signals can be important in equilibrium analyses. However, integral data did not prove useful when comparing signals from different types of oxygens, *i.e.* terminal oxygens relative to peroxide oxygens. Moreover, it proved difficult to compare the narrow peroxo signal with the broad peroxo signal, probably due to an underestimation of the latter signal. Therefore, any attempt to assign the narrow peroxo signal quantitatively failed. The equilibrium calculations and the dimerisation constants suggest that the speciation in the two media is very similar in pH areas where the contribution from medium anion containing complexes is negligible. The presence of the sulfate complexes,  $\text{MoX}_2\text{S}^{2-}/\text{MoX}_2\text{S}^-$  and the novel chloride complex,  $\text{MoX}_2\text{Cl}^-$ , demonstrates the ability of peroxomolybdates to attract ligands that would not have been coordinated to oxomolybdates under similar conditions.<sup>22</sup>

The lifetime of the  $\text{Mo}=\text{O}$  moiety in different species is in the order of  $10^{-3}$ – $10^{-2}$  s, somewhat longer for the  $\text{MoX}_2\text{S}$  species compared to  $\text{MoX}_2$  and  $\text{Mo}_2\text{X}_4$ . The protonation of the monomeric and dimeric complexes increase the rate of the chemical exchange of the  $\text{Mo}=\text{O}$  entity.

## Acknowledgements

This work has been financially supported by The Strategic Foundation (SSF), the Swedish Natural Science Research Council (NFR), the Hungarian Scientific Research Foundation (OTKA T 038296) and the European framework COST D12. We would like to thank Valeria Conte for supplying  $\text{H}_2^{17}\text{O}_2$ .

## References

1 K. M. Thompson, M. Spiro and W. P. Griffith, *J. Chem. Soc., Faraday Trans.*, 1996, 2535.

2 S. Campestrini, V. Conte, F. Di Furia and G. Modena, *J. Org. Chem.*, 1988, **53**, 5721.  
3 W. R. Thiel and T. Priermeier, *Angew. Chem., Int. Ed. Engl.*, 1995, **34**, 1737.  
4 O. Bortolini, L. Bragante, F. Di Furia and G. Modena, *Can. J. Chem.*, 1986, **64**, 1189.  
5 J. D. Lydon, L. M. Schwane and R. Thompson, *Inorg. Chem.*, 1987, **26**, 2606.  
6 F. Ghiron and R. Thompson, *Inorg. Chem.*, 1988, **27**, 4766.  
7 L. M. Schwane and R. Thompson, *Inorg. Chem.*, 1989, **28**, 3938.  
8 N. J. Campbell, A. C. Dengel, C. J. Edwards and W. P. Griffith, *J. Chem. Soc., Dalton Trans.*, 1989, 1203.  
9 J. Bailey, W. P. Griffith and B. C. Parkin, *J. Chem. Soc., Dalton Trans.*, 1995, 1833.  
10 R. Agnemo, *Proceedings of the 9th ISWPC*, Montréal, Canada, 1997, D2-1, ISBN 1-896742-14-9.  
11 V. Kubelka, R. C. Francis and C. W. Dence, *J. Pulp Paper Sci.*, 1992, **18**, J108.  
12 J. Jakara, A. Paren, J. Patola and T. Viitanen, *Pap. Puu*, 1994, **76**, 559.  
13 F. Taube, M. Hashimoto, I. Andersson and L. Pettersson, *J. Chem. Soc., Dalton Trans.*, 2002, 1002.  
14 M. S. Reynolds and A. Butler, *Inorg. Chem.*, 1996, **35**, 2378.  
15 M. Bonchio, V. Conte, F. Di Furia, G. Modena and S. Moro, *Inorg. Chem.*, 1993, **32**, 5797.  
16 W. P. Griffith, *J. Chem. Soc.*, 1964, 5248.  
17 F. Chauveau, P. Souchay and G. Tridot, *Bull. Soc. Chim. Fr.*, 1955, 1519.  
18 F. C. Palilla, N. Adler and C. F. Hiskey, *Anal. Chem.*, 1953, **25**, 926.  
19 Y. Schaeppi and W. D. Treadwell, *Helv. Chim. Acta*, 1948, **31**, 577.  
20 A. B. Filipov, G. A. Konishevskaya, V. M. Belusov and S. B. Grinenko, *Russ. J. Inorg. Chem.*, 1977, **22**, 180.  
21 E. Wendling, *Bull. Soc. Chim. Fr.*, 1965, 427.  
22 F. Taube, I. Andersson and L. Pettersson, in *Polyoxometalates: From Topology to Industrial Applications*, eds. M. T. Pope and A. Müller, Kluwer, Dordrecht, 2001, pp. 161–174.  
23 V. Conte, G. Miozzo and R. Salmaso, *Chim. Oggi*, 1989, **7**, 31.  
24 C. L. Perrin and T. J. Dwyer, *Chem. Rev.*, 1990, **90**, 183.  
25 N. Ingri, I. Andersson, L. Pettersson, A. Yagasaki, L. Andersson and K. Holmström, *Acta Chem. Scand.*, 1996, **50**, 717.  
26 M. Karlsson and J. Lindgren, personal communication.  
27 G. Eriksson, *Anal. Chim. Acta*, 1979, **112**, 375.  
28 J. M. Le Carpentier, A. Mitschler and R. Weiss, *Acta Crystallogr., Sect. B*, 1972, **28**, 1288.  
29 Mitschler, J. M. Le Carpentier and R. Weiss, *Chem. Commun.*, 1968, 1985.  
30 C. B. Shoemaker, D. P. Shoemaker and L. W. McAfee, *Acta Crystallogr., Sect. C*, 1985, **41**, 347.